Scaling behavior of the critical current density in $MgCNi_3$ microfibers

D. P. Young, M. Moldovan, and P. W. Adams
Department of Physics and Astronomy, Louisiana State University, Baton Rouge, Louisiana 70803, USA
(Received 3 May 2004; published 20 August 2004)

We present transport critical current measurements on microfibers consisting of a 80-nm thick layer of polycrystalline $MgCNi_3$ synthesized directly onto 7-μm diameter carbon fibers. Near the transition temperature T_c, the critical current density J_c is well described by the power law form $[1-(T/T_c)^2]^\alpha$, where $\alpha=2$ with no crossover to the Ginzburg-Landau exponent $\alpha=1.5$. We extrapolate $J_c(0)\approx 4\times 10^7$ A/cm^2, which is an order of magnitude greater than estimates obtained from magnetization measurements of polycrystalline powders. The field dependence is purely exponential $J_c(T,H)=J_c(T)\exp(-H/H_0)$ over the entire field range of 0 to 9 T. The unconventional scaling behavior of the critical current may be rooted in an anomalous temperature dependence of the London penetration depth.

DOI: 10.1103/PhysRevB.70.064508 PACS number(s): 74.25.Sv, 74.70.Ad, 74.78.Na

I. INTRODUCTION

The only known superconducting nonoxide perovskite $MgCNi_3$ has come under intense study since its discovery two years ago.[1] It is widely believed to be an important analog to the high-T_c perovskites by virtue of its chemical composition and its nonlayered cubic structure. One would hope that $MgCNi_3$ could help disentangle the influences of crystal symmetry, chemical doping, and micromorphology in its oxide cousins. Furthermore, band structure calculations have indicated that the superconducting phase of $MgCNi_3$ may, in fact, be near a ferromagnetic ground state, which is in accord with its high Ni content.[2] If this is indeed the case, then it would be related to the newly discovered nonconventional itinerate ferromagnetic superconductors UGe_2 (Ref. 3) and $ZrZn_2$.[4] Unfortunately, the volatility of Mg has hampered the synthesis of bulk crystalline samples of $MgCNi_3$ and, up to quite recently, only polycrystalline powders have been available.[5] Consequently, measurements of the transport and electron tunneling properties of the material have been compromised by poor sample morphology, making a quantitative characterization of the superconducting phase difficult. In the present report we present transport critical current measurements of annular $MgCNi_3$ fibers as a function of temperature and magnetic field. We show that that the scaling behavior near the transition temperature T_c is well described by a non-Ginzburg-Landau quadratic form[6] and that the overall magnitude of the zero-field critical current density $J_c(0)$ is in good agreement with that determined from estimates of the thermodynamic critical field H_c and the London penetration depth λ.[7] In addition, we show that the critical current is exponentially suppressed by axial magnetic field over the entire field range 0–9 T with no significant hysteresis. This behavior suggests that superconducting vortex pinning is weak in polycrystalline $MgCNi_3$.

II. SAMPLE PREPARATION

The annular $MgCNi_3$ fibers were formed by reacting Ni-coated carbon fibers in excess Mg vapor at 700 °C for 20–30 min in a vacuum sealed quartz tube. This process is similar to that used to form $MgCNi_3$ films, where CNi_3 precursor films were exposed to Mg vapor.[5] As is the case with the synthesis of films, the Mg exposure time was limited by the consumption of Mg via its reaction with the inner surface of the quartz tube. Exposures of several hours resulted in essentially bare carbon fibers. Presumably longer exposure times could be achieved by sealing the fibers in tubes made of a somewhat more less reactive material such as tantalum. This would allow a more systematic study of the effects of exposure time, oven temperature, and annealing schedule on the superconducting properties of the fibers. The Ni-coated carbon fibers used in this study were obtained from Novamet Specialty Products Corporation, under the product name Incofiber 12*K*20.[8] Incofiber 12*K*20 consists of 6–8 micron diameter carbon fibers which are coated with a 80-nm-thick film of Ni (99.97%) via a chemical vapor deposition process based on the high-temperature decomposition of $Ni(CO)_4$. This deposition method is ideal for the critical current studies described below in that it tends to produce quite uniform coatings and excellent adhesion. We also studied fibers in which the Ni coating was produced by an electrochemical deposition process and obtained similar results to the ones described below. Reliable annular contacts were made by applying Epotek conductive epoxy directly onto the reacted fibers. Critical currents of 3–5 mm long fibers were measured in a four-probe geometry using a standard pulsed technique. Currents were driven using pulse durations of 1–2 μs with a duty cycle of 1/1000, and the resulting voltages were measured via a boxcar integrator. Care was taken to ensure that the pulse width and duty cycle were low enough to avoid significant Joule heating at the contacts. The samples were cooled by vapor down to 1.8 K in magnetic fields up to 9 T via a Quantum Design PPMS.

III. RESULTS AND DISCUSSION

Shown in Fig. 1 is the low current density temperature dependence of the resistivity of a 7-μm diameter pristine Ni-coated fiber and a reacted fiber (see Fig. 1, inset). The resistivities have been normalized by their room-temperature values. Note the residual resistivity ratio of the Ni and the

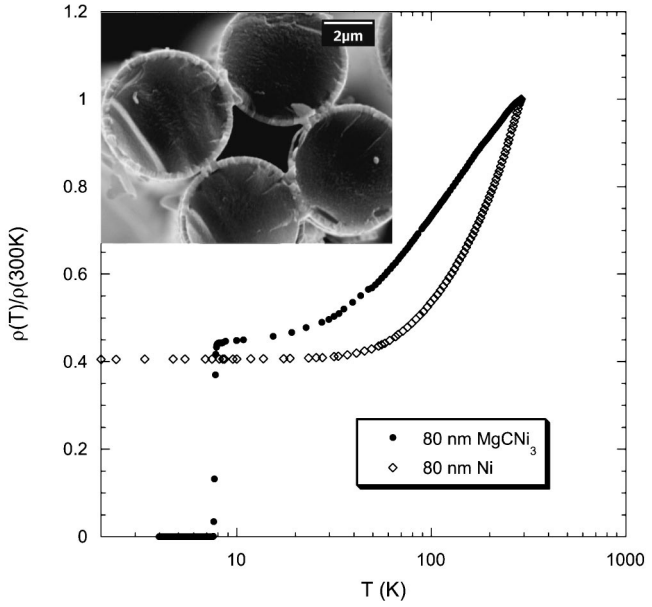

FIG. 1. Resistivity normalized by its room-temperature value as a function of temperature for a carbon fiber coated with 80 nm of Ni and a similar Ni-coated carbon fiber processed in Mg vapor to form an 80-nm $MgCNi_3$ sheath. Inset: Scanning electron micrograph of $MgCNi_3$ coated carbon fibers showing a cross-sectional view.

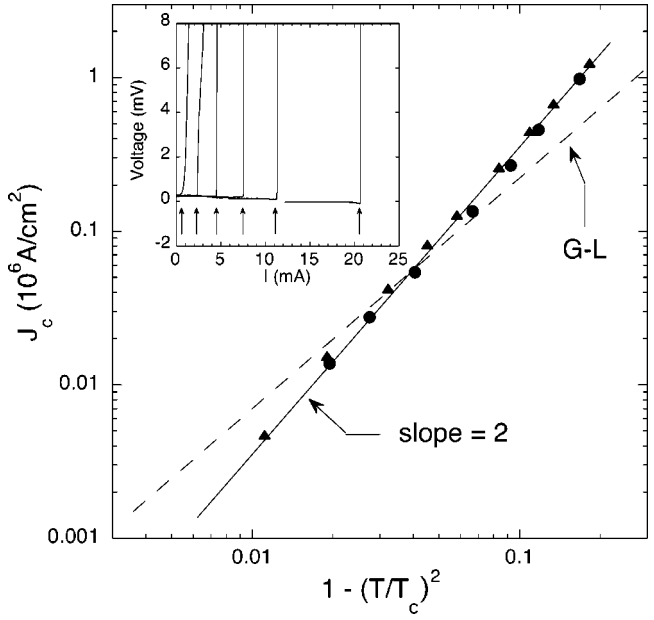

FIG. 2. Log-log plot of the scaling behavior of the critical current density near T_c in zero magnetic field for two 80-nm fibers. The solid line is provided as a guide to the eye and extrapolates to a zero-temperature density $J_c(0)=4\times10^7$ A/cm^2. The dashed line has the Ginzburg-Landau slope of 3/2. Inset: Typical *I-V* characteristics in zero field where the boxcar integrator output is plotted as a function of current pulse magnitude. The arrows depict the critical current thresholds at $T=7.45$, 7.3, 7.2, 7.1, 7.0, and 6.8 K, going from left to right.

$MgCNi_3$ fibers are comparable and that the normal state temperature dependence of the $MgCNi_3$ fibers appears to be logarithmic. The midpoint resistive transition temperature of the 80-nm-thick $MgCNi_3$ layer is $T_c=7.8$ K. This T_c is slightly higher than that of bulk powders and comparable to that recently reported in 60-nm-thick polycrystalline films on sapphire.[5] The 10-90 % resistive transition widths $\delta T_c/T_c \sim 2\%$ of the fibers are approximately 1/3 that of comparably thick planar films, and the extrapolated upper critical field $H_{c2}(0)\sim16.5$ T is somewhat higher than that of films $[H_{c2}(0)\sim13$ T$]$.[5] Critical current measurements were limited to temperatures above 5 K due to both the limitation of the electronics and the risk of damaging the samples. Shown in the inset of Fig. 2 are a set of typical *I-V* traces. The arrows depict the critical current thresholds used in the main body of the figure. The sharpness of the transitions, along with the ideal geometry of the samples, allow a much more precise determination of the temperature and field dependence of the critical current than could otherwise be extracted from critical-state modeling of magnetization hysteresis.[9] Furthermore, intergranular weak links in packed powder samples can greatly compromise the intrinsic critical current density. In Fig. 2 we present a log-log plot of the critical current density in zero magnetic field as a function of reduced temperature, where we have defined J_c by the onset of voltage as shown in the inset plot. The value of T_c used to scale the data in Fig. 2 was determined by the onset of voltage at $J=0.01J_c$. Care was taken to reduce the pulse width and duty cycle to the point were no hysteresis was observed across the critical current threshold. The dashed line in Fig. 2 is the Ginzburg-Landau (GL) critical current behavior for a homogeneous order parameter[6]

$$J_c=\frac{H_c(T)}{3\sqrt{6}\pi\lambda(T)}\propto[1-(T/T_c)^2]^{3/2}, \tag{1}$$

where H_c is the thermodynamic critical field and λ is the London penetration depth. Early critical current measurements on elemental films such as Sn and Pb showed good agreement with Eq. (1), with deviations attributed to edge effects.[10] Typically, the magnitude of the critical current density in elemental films is $J_c(0)>10^7$ A/cm^2. In order to rule out possible systematic errors arising from our technique, we measured the critical current behavior of a 200-nm-thick Pb film deposited via *e*-beam evaporation onto a 7-μm diameter rotating carbon fiber. The temperature dependence and the overall magnitude of the critical current of the Pb-coated fibers were found to be in good agreement with Eq. (1). Since the $MgCNi_3$ layer is only 80 nm thick, it is useful to consider the finite thickness modifications to Eq. (1). In particular, for very thin films of thickness $d<\lambda(0)$, the appropriate critical field[6] in Eq. (1) is $H_c^{\rm film}=\sqrt{24}H_c\lambda(T)/d$, which leads to a reduced temperature exponent of 1. Thus finite thickness effects tend to reduce the critical exponent from the bulk 3/2 value.

Significant deviations from the 3/2 exponent of Eq. (1) can arise from a number of sources. In particular, non-Ginzburg-Landau scaling behavior has been reported in many of the high-T_c systems, including La-Sr-Cu-O films,[11] Bi-Ca-Sr-Cu-O films,[12] oriented $YBa_2Cu_3O_{7-y}$ films,[13] and $YBa_2Cu_3O_7$ bicrystals.[14] The discrepancies have been mostly

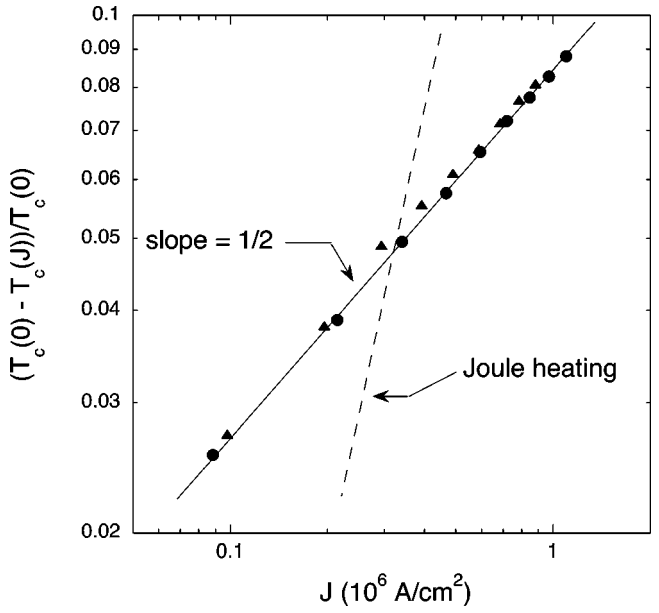

FIG. 3. Reduced transition temperature as a function of applied current density for the samples in Fig. 2. The dashed line has slope 2 and represents the effect of Joule heating.

attributed to weak links that are thought to be intrinsic to the complex granular microstructure of these ceramic materials. Observed temperature dependencies of the critical current in the high-T_c oxides are usually of the form $J_c(T)=J_c(0)(1-T/T_c)^{\alpha}$ near T_c, with α ranging between 1 and 2. **(**Note that near T_c, $[1-(T/T_c)^2]\sim 2(1-T/T_c)$.**)** Models of critical current behavior in granular systems assume that the intergrain transport is dominated by tunneling processes associated with either superconductor-insulator-superconductor (*SIS*) Josephson junctions.[15] or superconductor-normal-superconductor (*SNS*) proximity junctions.[16] The former is expected to produce a $(1-T/T_c)$ scaling and the latter $(1-T/T_c)^2$. Interestingly, granular systems can exhibit crossover behavior from one power law exponent to another.[17] For instance, evidence for *SIS* tunneling in thin YBCO films is seen in a critical current temperature dependence that evolves from the $\alpha=1$ of Josephson coupling to the Ginzburg-Landau $\alpha=3/2$ as one approaches T_c.[18] A similar crossover behavior can be induced by the application of a modest magnetic field ($\sim$0.01 T), where the GL scaling is recovered in finite field.[18]

The data in Fig. 2 show no evidence of crossover behavior, suggesting that the quadratic dependence is intrinsic and not an artifact of the micromorphology of the fibers. Furthermore, using the reported estimates of the zero-temperature thermodynamic field and penetration depth[7] $\mu_0 H_c(0)=0.22$ T and $\lambda(0)=220$ nm in Eq. (1), one obtains a reasonably large value of $J_c(0)\approx 4\times 10^7$ A/cm^2 which is in good agreement with the zero-temperature extrapolation of the data in Fig. 2. This suggests that the critical current magnitude is not compromised by weak links.

In Fig. 3 we have plotted the onset transition temperature shift as a function of current density. These data are presented as a consistency check of the $\alpha=2$ power law behavior in Fig. 2. The solid line is a guide to the eye and has the expected slope of 1/2. The dashed line represents the quadratic Joule heating dependence of which there is no indication in the data. If the anomalous scaling of Figs. 2 and 3 is, in fact, a property of the condensate, then it seems likely that it originates in the temperature dependence of the penetration depth in Eq. (1). In terms of GL theory,[6]

$$\lambda^2=\frac{m}{2\mu_0|\psi|^2e^2}, \tag{2}$$

where m is the electron mass, e the electron charge, μ_0 the vacuum permeability, and ψ the condensate wave function, whose square modulus is proportional to the density of Cooper pairs n_s. The theory assumes that near T_c, $|\psi|^2\propto(1-T/T_c)$. However, if the wave function couples to fluctuations of some other order parameter, such as that of a ferromagnetic phase, then critical behavior can be altered. In the case of $MgCNi_3$, it is believed that van Hove singularities in the Ni 3*d* bands may lead to paramagnon fluctuations that could influence the nature of the pairing.[2] The quadratic scaling behavior of the data in Fig. 2 is, in fact, consistent with a linear power law $\lambda\propto[1-(T/T_c)^2]$, in contrast to the square-root law of Eq. (2), perhaps supporting such a scenario. The case for an anomalous penetration depth in $MgCNi_3$ has recently been strengthened by low temperature measurements[19] in which a distinctly non-BCS quadratic temperature dependence is reported, $\lambda(T)\propto T^2$ for $T<T_c/4$. The T^2 dependence can be interpreted as evidence for a nodal gap structure such as that associated with *d*-wave superconductivity. However, the issue of the pairing state in $MgCNi_3$ remains controversial in that other probes such as electron tunneling and heat capacity are consistent with conventional BCS phonon-mediated superconductivity.[7,20] Nevertheless, there is still an open question as to whether or not a nearby ferromagnetic ground state exists, and, if so, to what extent it influences the superconducting properties of the system.

In Fig. 4 we plot the critical current density as a function of magnetic field at several different temperatures. The magnetic field was applied axially to the fibers. Note that the exponential field dependence exists over the entire field range. Though exponential suppression of J_c has also been reported in a number of high-T_c systems, they generally only show an exponential dependence over a limited field range. The solid lines are exponential fits to the data from which a characteristic field H_0 is extracted, see Fig. 4 inset. Interestingly, virtually no hysteresis in either field or current was observed during the course of these measurements, suggesting that flux pinning was not significant. In contrast, strong pinning effects have been reported in magnetization measurements of polycrystalline powders of $MgCNi_3$,[9] which have been attributed to superconducting vortex core pinning on intragrain graphite nanoprecipitates. It seems unlikely that the $MgCNi_3$ sheath on our fibers contains unreacted islands of carbon. We believe that since the reaction occurs in excess Mg vapor, carbon is leached out of the fiber to form $MgCNi_3$ at the correct stoichiometry until the nickel is completely consumed. The higher T_c's, sharp transitions, and higher

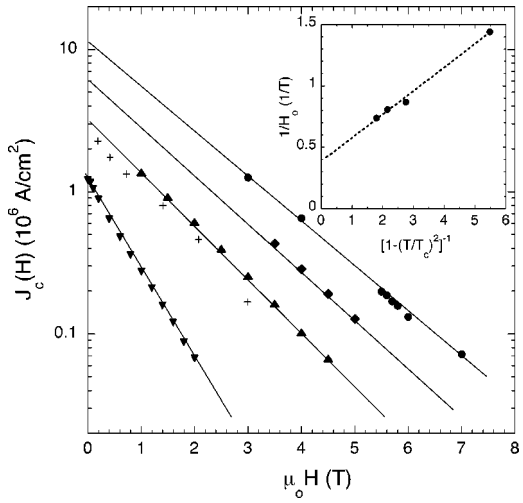

FIG. 4. Semi-log plot of the magnetic field dependence of the critical current density at several temperatures: ▼ 6.8 K, ▲ 6.0 K, ◆ 5.5 K, ● 5.0 K. The + symbols are 5.0 K data extracted from magnetization measurements of packed powder samples, Ref. 9. The field was applied longitudinally to the fiber. The solid lines represent exponential fits to the data from which a characteristic decay field H_0 is extracted. Inset: Inverse of characteristic field as a function of the inverse of the reduced temperature. The dashed line is provided as a guide to the eye.

critical fields of the fibers seem to support this scenario, providing further evidence that the anomalous critical current behavior is an intrinsic property.

The + symbols in Fig. 4 are critical current values obtained from the hysteretic behavior of the magnetization of $MgCNi_3$ powders[9] which also display an exponential dependence that is very similar to that of the transport data. This leads us to believe that the exponential behavior observed in both the powders and in our fibers is intrinsic to $MgCNi_3$. Interestingly, the packed powder values are approximately an order of magnitude smaller than the fiber values which is almost certainly a morphological effect. Obviously vortex dynamics may be playing a role in the field attenuation of J_c. Naively, one would expect that the Lorentz force on an axial, rectilinear vortex in the presence of a longitudinal current would be zero. However, it is known that the flux-line lattice becomes unstable against helical perturbations at sufficiently high supercurrent densities.[21] If such an instability leads to entanglement, then significant dissipation would be expected—possibly driving the system into a resistive state. How such a mechanism can lead to the field dependence of Fig. 4 and what the implications are for the vortex state in $MgCNi_3$ remains unclear. In the inset of Fig. 4 we plot the inverse of the characteristic field as a function of the inverse of the reduced temperature. The dashed line in the inset of Fig. 4 is a linear fit to the data which gives a slope whose value is approximately twice that of the intercept. The fit implies the following empirical expression for the temperature dependence of the characteristic field:

$$H_0(T) \approx 2.5\left[\frac{1 - T/T_c}{3/2 - T/T_c}\right], \tag{3}$$

where H_0 is in units of T. The linear scaling behavior of Eq. (3) may be related to that of the critical current. Interestingly, the asymptotic behavior of H_0 near T_c is the same as that of the thermodynamic critical field H_c. However, the magnitude of H_0 is much larger than H_c.

IV. CONCLUSION

In conclusion, the temperature and field dependence of the transport critical current in $MgCNi_3$ microfibers is well described by $J_c(T,H) = J_c(0)[1-(T/T_c)^2]^2 \exp[-(H/H_0)]$, where $J_c(0) \approx 4 \times 10^7$ A/cm^2. We believe that the non-Ginzburg-Landau exponent is not a morphological effect and that it may be reflective of the anomalous penetration depth behavior recently reported in polycrystalline powders.[19] Whether or not the anomalous temperature dependence of the London penetration depth can be attributed to a nonconventional superconductivity in $MgCNi_3$ remains controversial. But even if the superconducting state is conventional, the critical behavior of $MgCNi_3$, as manifest through the critical current scaling, is not.

ACKNOWLEDGMENTS

We gratefully acknowledge discussions with Dana Browne, Ilya Vekhter, Milind Kunchur, and Lisa Podlaha. This work was supported by the National Science Foundation under Grant No. DMR 02-04871 and the LEQSF under Grant No. 2001-04-RD-A-11.

[1] T. He, Q. Huang, A.P. Ramirez, Y. Wang, K.A. Regan, N. Rogado, M.A. Hayward, M.K. Haas, J.S. Slusky, K. Inumara, H.W. Zandbergen, N.P. Ong, and R.J. Cava, Nature (London) **411**, 54 (2001).

[2] H. Rosner, R. Weht, M.D. Johannes, W.E. Pickett, and E. Tosatti, Phys. Rev. Lett. **88**, 027001 (2002); S. B. Dugdale and T. Jarlborg, Phys. Rev. B **64**, 100508 (2001).

[3] S.S. Saxena, K. Ahilan, F.M. Grosche, R.K.W. Haselwimmer, M.J. Steiner, E. Pugh, I.R. Walker, S.R. Julian, P. Monthoux, G.G. Lonzarich, A. Huxley, I. Sheikin, D. Braithwaite, and J. Flouquet, Nature (London) **406**, 587 (2000).

[4] C. Pfleiderer, M. Uhlarz, S.M. Hayden, R. Vollmer, H. von Lohneysen, N.R. Bernhoeft, and G.G. Lonzarich, Nature (London) **412**, 58 (2001).

[5] D.P. Young, M. Moldovan, D.D. Craig, P. W. Adams, and Julia Y. Chan, Phys. Rev. B **68**, 020501 (2003).

[6] M. Tinkam, *Introduction to Superconductivity* (McGraw-Hill, New York, 1996).

[7] Z.Q. Mao, M.M. Rosario, K.D. Nelson, K. Wu, I.G. Deac, P. Schiffer, Y. Liu, T. He, K.A. Regan, and R.J. Cava, Phys. Rev. B **67**, 094502 (2003); S.Y. Li, R. Fan, X.H. Chen, C.H. Wang, W.Q. Mo, K.Q. Ruan, Y.M. Xiong, X.G. Luo, H.T. Zhang, L. Li,

Z. Sun, and L.Z. Cao, *ibid.* **64**, 132505 (2001).
[8] Novamet Speciality Products Corporation, 681 Lawlins Road, Wyckoff, NJ 07481 (www.novametcorp.com).
[9] L.D. Cooley, X. Song, J. Jiang, D.C. Larbalestier, T. He, K.A. Regan, and R.J. Cava, Phys. Rev. B **65**, 214518 (2002).
[10] W.J. Skocpol, Phys. Rev. B **14**, 1045 (1976); T.K. Hunt, Phys. Rev. **151**, 325 (1966).
[11] K. Moriwaki, Y. Enomoto, and T. Murakami, Jpn. J. Appl. Phys. **26**, L521 (1986).
[12] K. Setsune, K. Hirochi, H. Adachi, Y. Ichikawa, and K. Wasa, Appl. Phys. Lett. **53**, 600 (1988); H.E. Horng, J.C. Jao, H.C. Chen, H.C. Yang, H.H. Sung, and F.C. Chen, Phys. Rev. B **39**, 9628 (1989).
[13] W. Widder, L. Bauernfeind, H.F. Braun, H. Burkhardt, D. Rainer, M. Bauer, and H. Kinder, Phys. Rev. B **55**, 1254 (1997); S.B. Ogale, D. Dijkkamp, T. Venkatesan, X.D. Wu, and A. Inam, *ibid.* **36**, 7210 (1987).
[14] D. Dimos, P. Chaudhari, and J. Mannhart, Phys. Rev. B **41**, 4038 (1990).
[15] V. Ambegaokar and A. Baratoff, Phys. Rev. Lett. **10**, 486 (1963).
[16] P.G. De Gennes, Rev. Mod. Phys. **36**, 225 (1964).
[17] J.R. Clem, B. Bumble, S.I. Raider, W.J. Gallagher, and Y.C. Shih, Phys. Rev. B **35**, 6637 (1987).
[18] H. Darhmaoui and J. Jung, Phys. Rev. B **53**, 14 621 (1996).
[19] R. Prozorov, A. Snezhko, T. He, and R.J. Cava, Phys. Rev. B **68**, 180502 (2003).
[20] J.Y. Lin, H.D. Yang, and C.Q. Jin, Physica C **388**, 559 (2003); P.M. Singer, T. Imai, T. He, M.A. Hayward, and R.J. Cava, Phys. Rev. Lett. **87**, 257601 (2001); G. Kinoda, M. Nishiyama, Y. Zhao, M. Murakami, N. Koshizuka, and T. Hasegawa, Jpn. J. Appl. Phys. **40**, L1365 (2001); J.H. Shim, S.K. Kwon, and B.I. Min, Phys. Rev. B **64**, 180510 (2001).
[21] E.H. Brandt, Phys. Rev. B **25**, 5756 (1982).